High-frequency stimulation produces a transient blockade of voltage-gated currents in subthalamic neurons.

Corinne Beurrier, Bernard Bioulac, Jacques Audin, Constance Hammond

High-Frequency Stimulation Produces a Transient Blockade of Voltage-Gated Currents in Subthalamic Neurons

CORINNE BEURRIER,[1] BERNARD BIOULAC,[1] JACQUES AUDIN,[1] AND CONSTANCE HAMMOND[2]
[1]*Laboratoire de Neurophysiologie, Centre National de la Recherche Scientifique, Unite Mixte de Recherche 5543, Université Bordeaux II, 33076 Bordeaux Cedex; and* [2]*Institut National de la Santé et de la Recherche Médicale U29, 13273 Marseille Cedex 09, France*

Received 8 June 2000; accepted in final form 22 December 2000

Beurrier, Corinne, Bernard Bioulac, Jacques Audin, and Constance Hammond. High-frequency stimulation produces a transient blockade of voltage-gated currents in subthalamic neurons. *J Neurophysiol* 85: 1351–1356, 2001. The effect of high-frequency stimulation (HFS) of the subthalamic nucleus (STN) was analyzed with patch-clamp techniques (whole cell configuration, current- and voltage-clamp modes) in rat STN slices in vitro. A brief tetanus, consisting of 100-μs bipolar stimuli at a frequency of 100–250 Hz during 1 min, produced a full blockade of ongoing STN activity whether it was in the tonic or bursting mode. This HFS-induced silence lasted around 6 min after the end of stimulation, was frequency dependent, could be repeated without alteration, and was not synaptically induced as it was still observed in the presence of blockers of ionotropic GABA and glutamate receptors or in the presence of cobalt at a concentration (2 mM) that blocks voltage-gated Ca^{2+} channels and synaptic transmission. During HFS-induced silence, the following alterations were observed: the persistent Na^+ current (I_{NaP}) was totally blocked (by 99%), the Ca^{2+}-mediated responses were strongly reduced including the posthyperpolarization rebound (−62% in amplitude) and the plateau potential (−76% in duration), suggesting that T- and L-type Ca^{2+} currents are transiently depressed by HFS, whereas the Cs^+-sensitive, hyperpolarization-activated cationic current (I_h) was little affected. Thus a high-frequency tetanus produces a blockade of the spontaneous activities of STN neurons as a result of a strong depression of intrinsic voltage-gated currents underlying single-spike and bursting modes of discharge. These effects of HFS, which are completely independent of synaptic transmission, provide a mechanism for interrupting ongoing activities of STN neurons.

INTRODUCTION

The observation that deep brain stimulation applied at a high-frequency (HFS) in the subthalamic nucleus (STN) and its surgical destruction, both greatly ameliorate motor signs of Parkinson's disease in patients, led to the hypothesis that HFS blocks, partly or completely, the activity of STN neurons. In keeping with this, HFS in the STN has been shown to significantly decrease the frequency of extracellularly recorded STN neurons in rats in vivo (Benazzouz et al. 1997). As STN neurons are glutamatergic excitatory output neurons (Hammond et al. 1978; Robledo and Féger 1990; Smith and Parent 1988), the immediate consequence of their reduction of activity could be the decrease of activity in target nuclei [substantia nigra pars reticulata (SNr) and entopeduncular nucleus/globus pallidus internal part (EP/GPi)] as observed in 1-methyl-4-phenyl-1,2,3,6-tetrahydropyridine (MPTP)-treated monkeys and naive rats (Benazzouz et al. 1995; Burbaud et al. 1994; Hayase et al. 1996). It has also been suggested that the consequence of clinical HFS will be to somehow counteract the abnormal bursting pattern recorded in the STN in animal models of Parkinson disease (Bergman et al. 1994; Hassani et al. 1996; Hollerman and Grace 1992; Vila et al. 2000).

To understand the contribution of HFS in pathological conditions, it is clearly essential to determine whether a HFS of the STN could modify or block the intrinsic activities of STN neurons and to analyze the underlying mechanisms. This is best achieved in vitro, as slice preparations enable to better isolate the various effects of a tetanus on neuronal properties. In the present study, using patch-clamp recordings of rat STN neurons in slices, we report that HFS of the STN suppresses the spontaneous activity of both single-spike and bursting STN neurons. The effects of HFS are synaptic-independent and are mediated by a blockade of the voltage-gated currents and particularly the persistent Na^+ (I_{NaP}) current and the L- and T-type Ca^{2+} currents (I_{CaL} and I_{CaT}) that are known to generate the intrinsic spontaneous discharge modes of STN neurons (Beurrier et al. 1999, 2000; Bevan and Wilson 1999).

METHODS

Slice preparation

Experiments were performed on STN neurons in slices obtained from 20- to 28-day-old male Wistar rats. Rats were anesthetized with ether and decapitated. The brain was quickly removed, and a block of tissue containing the STN was isolated on ice in a 0–5°C oxygenated solution containing (in mM) 1.15 NaH_2 PO_4, 2 KCl, 26 $NaHCO_3$, 7 $MgCl_2$, 0.5 $CaCl_2$, 11 glucose, and 250 saccharose, equilibrated with 95% O_2-5% CO_2 (pH 7.4). This cold solution, with a low NaCl and $CaCl_2$ content, improved tissue viability. In the same medium, 300- to 400-μm-thick coronal slices were prepared using a vibratome (Campden Instruments, Loughborough, UK) and were then incubated at room temperature in a Krebs solution containing (in mM) 124 NaCl, 3.6 KCl, 1.25 *N*-[2-hydroxyethyl]piperazine-*N*′-[2-ethanesulfonic acid] (HEPES), 26 $NaHCO_3$, 1.3 $MgCl_2$, 2.4 $CaCl_2$, and 10 glucose, equilibrated with 95% O_2-5% CO_2 (pH 7.4). After a 2-h recovery period, STN slices were transferred individually to an interface-type

Address for reprint requests: C. Hammond, INSERM U29, Route de Luminy, 13273 Marseille Cedex 09, France (E-mail: hammond@inmed.univ-mrs.fr).

The costs of publication of this article were defrayed in part by the payment of page charges. The article must therefore be hereby marked "*advertisement*" in accordance with 18 U.S.C. Section 1734 solely to indicate this fact.

recording chamber, maintained at 30 ± 2°C (mean ± SD) and continuously superfused (1–1.5 ml/min) with the oxygenated Krebs solution.

STN stimulation

The stimulating electrode was positioned in the middle of the STN identified as an ovoid structure just lying at the border of the basal part of the cerebral peduncle. Two types of stimulating electrodes were tested: The bipolar concentric electrode measuring 0.5 mm in diameter (NEX-100, Rhodes Medical Instruments) used by Burbaud (Burbaud et al. 1994) and Benazzouz (Benazzouz et al. 1995) for the in vivo stimulation of the rat STN and a much thinner electrode (0.01 mm in diameter) that we designed to avoid any mechanical lesion of the STN.

Electrophysiological recordings

Slices were visualized using a dissecting microscope and the recording electrode was precisely positioned in the STN. Electrophysiological recordings of STN neurons were performed in the current- or voltage-clamp mode using the blind patch-clamp technique in the whole cell configuration. Patch electrodes were pulled from filamented borosilicate thin-wall glass capillaries (GC150F-15, Clarck Electromedical Instruments, Pangbourne, UK) with a vertical puller (PP-830, Narishige, Japan) and had a resistance of 10–12 MΩ when filled with the following (in mM): 120 Kgluconate, 10 KCl, 10 NaCl, 10 ethylene glycol-bis(b-aminoethyl ether)-*N*,*N*,*N*′,*N*′-tetraacetic acid (EGTA), 10 HEPES, 1 $CaCl_2$, 2 MgATP, and 0.5 NaGTP, pH 7.25.

Reagents

Drugs were applied by bath. Reagents were procured from Sigma (St. Louis, MO), except 6-cyano-7-nitroquinoxaline-2,3-dione (CNQX), D-(−)-2-amino-5-phosphopentanoic acid (D-APV), and bicuculline, which were purchased from Tocris (Bristol, UK).

Data analysis

Membrane potential was recorded using Axoclamp 2A or Axopatch 1D amplifier (Axon Instruments, Foster City, CA), displayed simultaneously on a storage oscilloscope and a four-channel chart recorder (Gould Instruments, Longjumeau, France), digitized (DR-890, Neuro-Data Instruments, New York), and stored on a videotape for subsequent off-line analysis. During voltage-clamp recordings, membrane currents were fed into an A/D converter (Digidata 1200, Axon Instruments), stored, and analyzed on a PC using pCLAMP software (version 6.0.3, Axon Instruments). Corrections for the liquid junction potential were performed according to Neher (1992): −6 mV for the K-gluconate-based pipette solution as estimated with a 3 M KCl ground electrode.

RESULTS

HFS-induced arrest of single-spike or bursting activity

STN activity was recorded in current-clamp mode (whole cell configuration) for at least 1 min before the HFS was applied. Using a bipolar concentric stimulating electrode similar to that used in rat in vivo (see METHODS), a brief (1 min) HFS consisting of 100 μs stimuli of 5–8 V amplitude, produced a blockade of ongoing activity whether it was in single-spike (Fig. 1) or bursting (Fig. 2) mode. This effect was frequency dependent (Figs. 1*A* and 2) with an optimal frequency of 166 up to 250 Hz that produced a full blockade of the activity ($n = 17$). The latency of the HFS-induced silence could not be determined in detail as during the 1-min stimulation period, artifacts prevented analysis of the activity. Nevertheless as shown in Figs. 1*B* and 2, above a certain frequency, the onset of the blockade was immediately obvious by the end of the train. Interestingly, HFS blocked both single spike (Fig. 1) and burst firing (Fig. 2) modes, suggesting that its mechanisms do not involve a current(s) that is expressed only in one type of discharge.

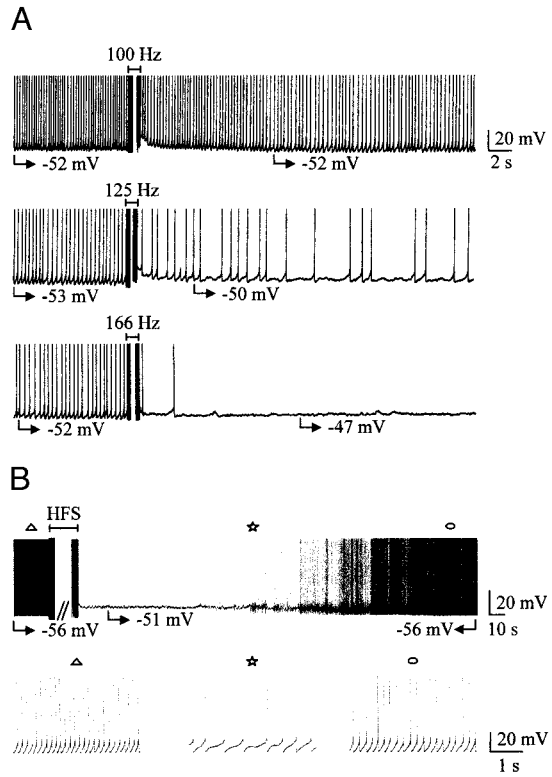

FIG. 1. Effect of high-frequency stimulation (HFS) on the spontaneous single-spike activity of 2 subthalamic nucleus (STN) neurons. *A*: frequency dependence of HFS. Applied at 100 Hz, HFS had nearly no posteffect whereas at 125 Hz it decreased the frequency of tonic activity and at 166 Hz stopped single-spike activity for 5 min. *B*: continuous chart recording (*top*) at slow time resolution of the activity of an other STN neuron. HFS (250 Hz) stopped single-spike activity at a potential of −51 mV for 1 min 12 s. Symbols indicate the parts of the top recording that are shown at an expanded time scale in *bottom traces*.

The suppression of STN spontaneous activity was observed for 5.8 ± 0.7 min (range: 1.1–18.0, $n = 31$) after HFS. At the end of the silence period, spontaneous activity slowly recovered in the same mode as before stimulation (Figs. 1*B* to 6). During cell silence, membrane potential remained stable at −52.2 ± 0.8 mV (range: −40 to −68, $n = 45$) for tonic cells and at −56.2 ± 1.4 mV (range: −48 to −61 mV, $n = 8$) for bursting cells. These membrane potentials were significantly more depolarized than the potentials at which cells were silent in control conditions: before HFS, cells tested in the tonic mode were silent at −60.2 ± 0.6 mV (range: −49 to −68 mV, $n = 45$, $P < 0.001$, paired *t*-test) and cells tested in the bursting mode were silent at −63.5 ± 1.3 mV (range: −56 to −68 mV, $n = 8$, $P = 0.015$, paired *t*-test). This suggested that HFS did not stop STN cell activity simply by transiently hyperpolarizing the membrane.

Spikes could still be evoked during the silence period in all tested neurons ($n = 60$). However, in half of the cells, spike threshold was significantly higher during the silence period

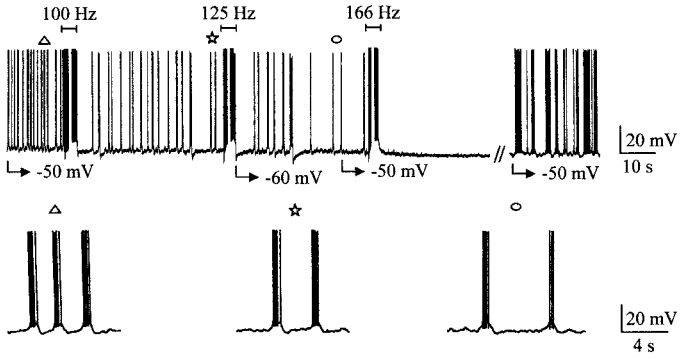

FIG. 2. Frequency-dependent effect of HFS on spontaneous bursting activity of a STN neuron. Chart recording at slow time base of a bursting STN neuron (burst firing was evoked by continuous injection of −150 pA). At 100 and 125 Hz, HFS decreased burst frequency (*bottom traces*) whereas at 166 Hz it totally suppressed bursting activity for 1 min and 49 s. Activity then recovered in burst firing mode. Symbols indicate the parts of the *top recording* that are shown at an expanded time scale in *bottom traces.*

(−39.3 ± 1.6 mV, $n = 30$) compared with the control (−47.5 ± 0.6 mV, $n = 30$, $P < 0.001$; Fig. 3). So was also input membrane resistance, which was significantly increased during HFS-induced silence, when tested at $V_m = -65$ mV by applying hyperpolarizing current pulses of −100/-200 pA amplitude (247.2 ± 21.1 vs. 226.1 ± 16.3 MΩ, $P = 0.035$, $n = 20$). A second tetanus, applied after the cell recovered from the first one, reversibly silenced the cell again ($n = 15$). This could be repeated as long as patch recording could last. Therefore HFS does depress neuronal activity in slices, and this effect is short lasting and can be repeated. In subsequent experiments, we used a thinner electrode designed to avoid any mechanical lesion of the STN. We chose to use the same parameters of train duration (1 min) and of bipolar stimuli intensity (5–8 V) and duration (100 μs) but to vary their frequency in the train (range 100–500 Hz) to obtain a clear-cut suppression of activity during which a long-lasting analysis of currents or specific responses could be performed.

HFS-induced suppression of activity is independent of synaptic activity

An important issue was to determine whether effects of the train were mediated by synaptic transmission. Bath applica-

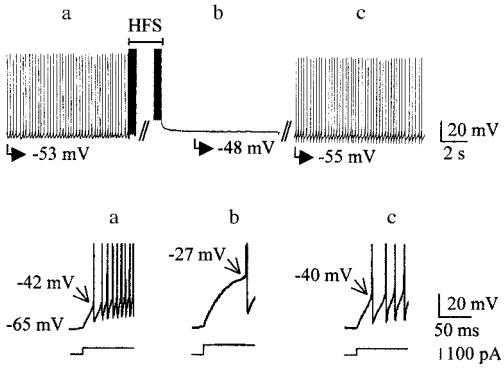

FIG. 3. Increase of threshold potential for Na^+-dependent spikes during HFS-induced silence. Chart recording at low time base of a tonic STN neuron (*top*). HFS (250 Hz) stopped single-spike activity at a potential of −48 mV for 1 min 25 s. *Bottom*: Na^+-dependent spikes evoked by a depolarizing pulse of 100 ms, before HFS (*a*, 80 pA), during HFS-induced silence (*b*, 100 pA), and after recovery of activity (*c*, 80 pA).

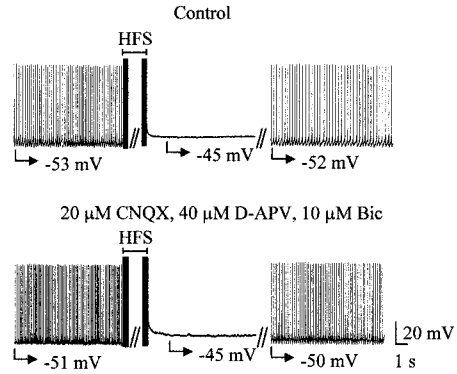

FIG. 4. HFS-induced silence is independent of ionotropic synaptic transmission. HFS (500 Hz) reversibly stopped single-spike activity of a STN neuron for 8 min at −45 mV (control). A 2nd HFS (500 Hz) was applied in the continuous presence of D-APV, CNQX, and bicuculline (Bic). Single-spike activity was stopped at −45 mV for 9 min.

tions of ionotropic glutamate and $GABA_A$ receptor antagonists, CNQX (20 μM), D-APV (40 μM), and bicuculline (10 μM) failed to prevent the effects of HFS ($n = 6$, Fig. 4). Furthermore HFS still suppressed single-spike activity when synaptic transmission was blocked by 2 mM Co^{2+} ($n = 16$, Fig. 5*A*, *top*). Since the silencing effect of HFS did not require Ca^{2+}-dependent transmitter release, we tested whether it was possible to mimic this effect with intracellular stimulation of the recorded cell. When comparing the two types of HFS (extracellular and intracellular) in the same tonically active STN neurons ($n = 8$), it appeared that both HFS resulted in a silence of the cell. However, intracellular HFS had a different effect on membrane potential: there was a strong hyperpolarization of the membrane at the break of the intracellular pulses (to −63.2 ± 3.1 mV) that declined in about 20 s to −48.1 ± 4.1 mV, a potential at which tonic activity recovered ($n = 8$, data not shown). Such an after hyperpolarization and slow membrane repolarization were never observed after extracellular HFS where membrane potential remained stable during cell silence (Figs. 1–6).

HFS-induced decrease of voltage-gated currents

We hypothesized that HFS induced a modification of voltage-sensitive currents essential for the expression of tonic and burst-firing modes (Beurrier et al. 2000; Bevan and Wilson 1999). In the tonic mode, the silencing effect of HFS did not require Ca^{2+} influx since it was still observed in the presence of 2 mM Co^{2+} nor increase of intracellular Ca^{2+} concentration since it was present in BAPTA-loaded cells ($n = 4$, data not shown). We therefore tested the effect of HFS on spontaneous tonic activity and I_{NaP} recorded from the same STN neurons by shifting from current- to voltage-clamp mode before, during, and after HFS-induced silence. In voltage-clamp mode, in response to a voltage ramp and in the continuous presence of Co^{2+}, a TTX-sensitive inward current that had the characteristics of a persistent Na^+ current was recorded. It was strongly reduced during HFS-induced silence (Fig. 5). *I-V* relationships before and during HFS-induced silence showed that peak amplitude of I_{NaP} was reduced by 99% during cell silence as compared with the control (from −122.2 ± 13.1 to −1.1 ± 1.1 pA, $n = 9$; Fig. 5, *B* and *C*). This effect reversed to 78% of control (to −92.5 ± 9.9 pA, $n = 8$) once cell activity recov-

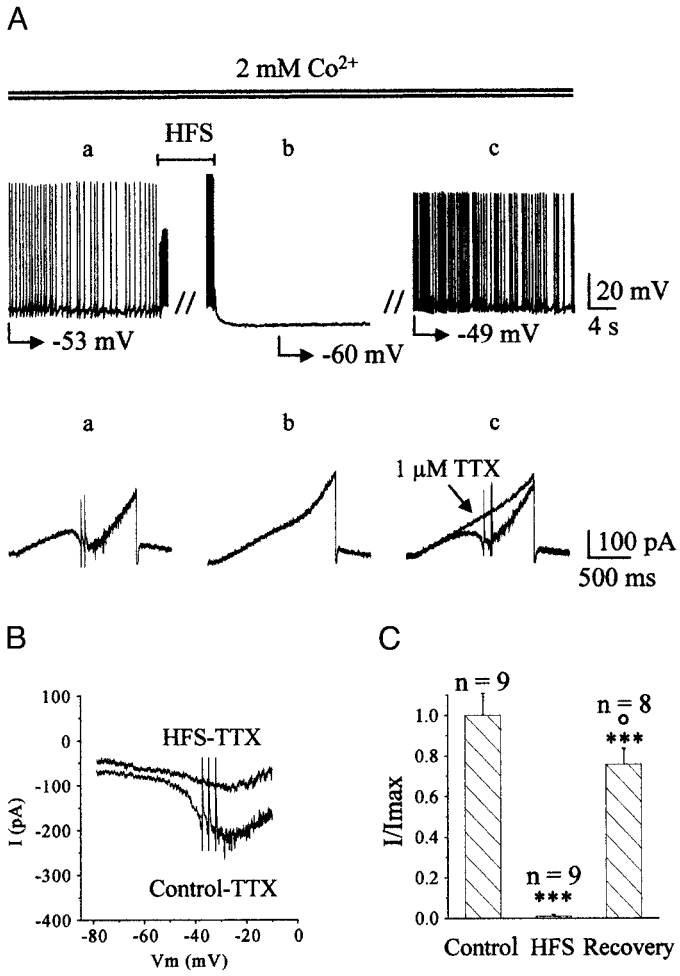

FIG. 5. Effect of HFS on the persistent Na^+ current in the absence of synaptic transmission. *A*: HFS (500 Hz) applied in the continuous presence of Co^{2+} (2 mM) stopped the activity of a tonically firing STN neuron (for 18 min at −60 mV; *top*). In response to a 5-mV/s depolarizing ramp from −80 to −10 mV, a slow inward current was recorded before HFS (*a*), 110 s after HFS (*b*, during HFS-induced silence), and 36 min after HFS (*c*, after recovery of activity). TTX (1 μM) applied at the end of the experiment totally abolished the slow inward current as well as the fast ones (*c*, *bottom*). *B*: *I-V* relationships of the persistent Na^+ current obtained from the same cell in *A*. The curve HFS-TTX represents the subtraction of traces *Ab–Ac*. The curve control-TTX represents the subtraction of traces *Aa–Ac*. *C*: histogram of I_{NaP} peak amplitude before (control), during (HFS), and after (recovery) HFS-induced silence. *, comparison with preceding column; ○, comparison with control. * or ○: $P < 0.05$; **: $P < 0.001$; ***: $P < 0.0001$.

ered. When applied at the end of the experiment, TTX (1 μM) totally blocked this current, confirming that it was I_{NaP} (Fig. 5*A*).

Spontaneous bursting mode and I_{Ca} were then analyzed. However, since the recording of Ca^{2+} currents requires the presence of K^+ channel blockers, a procedure incompatible with the recording of burst firing in current-clamp mode, the amplitude of Ca^{2+} currents was therefore evaluated from the evoked potentials they underlie: the rebound depolarization, also called low-threshold Ca^{2+} spike (LTS), that results from the activation of a T-type Ca^{2+} current and the plateau potential that results from the combined action of the nifedipine-sensitive L-type Ca^{2+} current and a Ca^{2+}-activated inward current (Beurrier et al. 1999). Following HFS, during minutes of silence, plateau duration was reduced by 62% (from 1119.4 ± 150.6 to 425.6 ± 111.4 ms, $n = 32$) sometimes with a total suppression of the after spike depolarization (Fig. 6, *A*, *top* and *middle*, and *B*, *left*). Concomitantly, the amplitude of the rebound potential was reduced by 75.9% (from 8.8 ± 0.4 to 2.1 ± 0.5 mV, $n = 23$; Fig. 6, *A*, *top* and *bottom*, and *B*, *right*). Once cell activity recovered, the effects on plateau potential duration and on the amplitude of rebound potential reversed to 66% of control (to 739.4 ± 217.9 ms, $n = 18$) and to 39% of control (to 3.4 ± 0.8 mV, $n = 14$), respectively.

In contrast, the Cs^+-sensitive, hyperpolarization-activated cation current (I_h) was not affected by HFS at potentials normally traversed by the membrane during tonic firing. It was

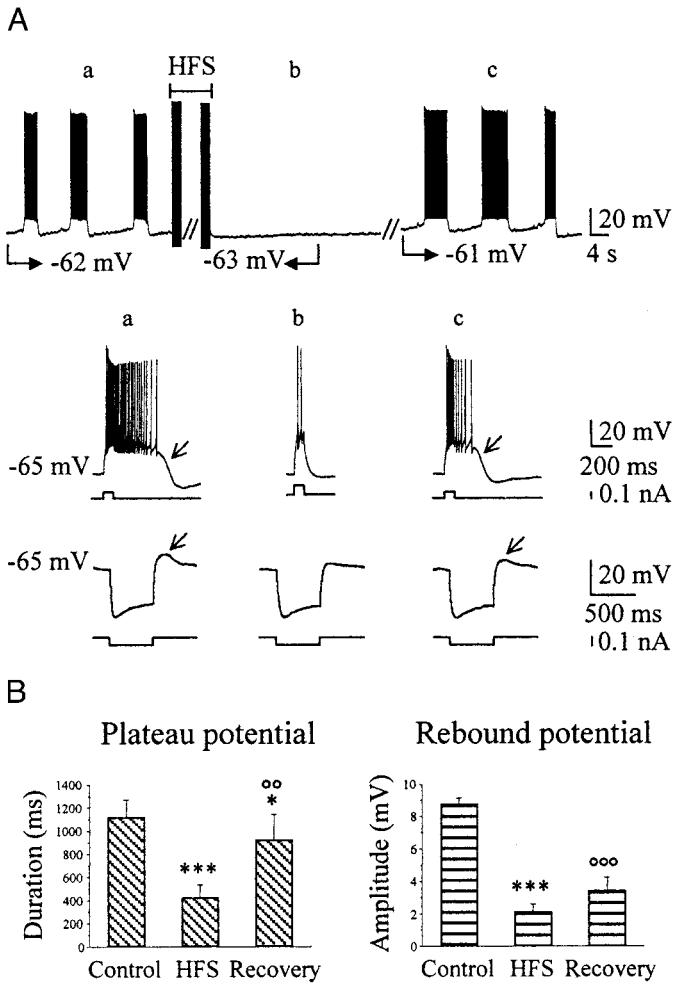

FIG. 6. Effect of HFS on Ca^{2+}-mediated responses. *A*, *top*: HFS (500 Hz) stopped the activity of a burst-firing STN neuron (at −63 mV). *Middle*: plateau potential triggered by a depolarizing current pulse at $V_m = -65$ mV (+80 pA, 100 ms), lasted 760 ms before HFS (*a*), lasted 150 ms during cell silence (*b*, 70 s after HFS), and lasted 520 ms during recovery of bursting activity (*c*, 17 min after HFS). ↓ indicates the after spike depolarization (ADP) present in *a* and *c* and absent in *b*. *Bottom*: rebound potential (↓) recorded at the break of a hyperpolarizing pulse (−80 pA, 500 ms) had an amplitude of 10 mV before HFS (*a*), of 2.5 mV during silence (*b*, 8 min 30 s after HFS), and of 5 mV after recovery of bursting activity (*c*, 34 min after HFS). In the same traces, note the absence of modification of the depolarizing sag that developed during the current pulse. All recordings were obtained from the same STN neuron. *B*, *left*: histogram of plateau potential duration before (control), during (HFS), and after (recovery) HFS-induced silence. *Right*: histogram of rebound potential amplitude before, during, and after HFS-induced silence. *, comparison with preceding column; ○, comparison with control. *$P < 0.05$; ** or ○○: $P < 0.001$; *** or ○○○: $P < 0.0001$.

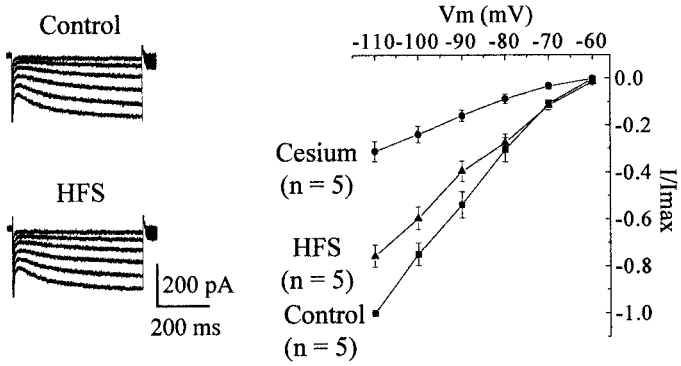

FIG. 7. Effect of HFS on the hyperpolarization-activated cation current I_h. *Left*: from a holding potential of −50 mV, a family of currents was evoked in response to 1,500-ms hyperpolarizing steps from −60 to −110 mV (10-mV increment) before HFS (control) and during HFS-induced silence (HFS). *Right*: *I-V* relationship of I_h before (control), during HFS-induced silence (HFS), and in the presence of 1–3 mM cesium in the bath (V_H = −50 mV). Values of *I* were obtained by subtracting the value of the current at the beginning of the hyperpolarizing pulse from that at the end of the pulse. Currents were normalized (I/I_{max}) to the maximal current (I_{max}) recorded at −110 mV.

reduced between −80 and −110 mV (by 26.5% at −90 mV, n = 5, Fig. 7). Consistent with these findings on I_h, the amplitude of the depolarizing sag observed during a hyperpolarizing current pulse was not significantly affected (it was reduced by 4.8%, from 5.21 ± 0.82 to 4.99 ± 0.80 mV, P = 0.69, n = 12; Fig. 6*A*, *bottom*).

DISCUSSION

Our results show that HFS blocks the spontaneous activity of tonic and bursting STN neurons with a mechanism that does not require Ca^{2+}-dependent transmitter release. The silencing effect of HFS has a short latency, is brief, reversible, can be repeated several times with little change, and is frequency dependent. It is mediated by a dramatic reduction of Na^+ and Ca^{2+} voltage-gated currents leading to an interruption of the spontaneous activities of the neurons. In fact, in single-spike activity, a TTX-sensitive, persistent Na^+ current (I_{NaP}), underlies the slow pacemaker depolarization that spontaneously depolarizes the membrane from the peak of the after spike hyperpolarization to the threshold potential for spike initiation (Beurrier et al. 2000; Bevan and Wilson 1999). In contrast, in burst-firing mode, the interplay between a T-type Ca^{2+} current (I_{CaT}), an L-type Ca^{2+} current (I_{CaL}), and a Ca^{2+}-activated inward current, all insensitive to TTX, underlie recurrent membrane oscillations (Beurrier et al. 1999). The blockade of these subliminal currents can also explain the increase of membrane resistance observed during HFS-induced silence.

The silencing effect of HFS does not result from the activation of a local network and is not mediated by the stimulation of afferents to the STN, since it was still observed in the presence of blockers of glutamatergic and GABAergic ionotropic synaptic transmission and in the presence of cobalt at a concentration that totally blocked synaptic transmission in the STN. It was in fact reproduced by direct stimulation of the recorded STN cell as previously tested by Borde et al. (2000) in hippocampal CA1 pyramidal neurons. In this preparation, a low-frequency intracellular stimulation induced a depression of activity that developed rapidly, was reversible, persisted up to 3 min and was still observed when synaptic transmission was strongly reduced by the P-type Ca^{2+} channel blocker ω-agatoxin IVA or enhanced by 4-aminopyridine. The insensitivity of depression to synaptic blockade indicates little if any involvement of synaptic mechanisms and implies that postsynaptic mechanisms are key factors as observed in the present study with extracellular HFS. However, mechanisms underlying intracellular stimulation may be different from those underlying extracellular HFS. The silencing effect of intracellular stimulation is Ca^{2+}-dependent since it requires Ca^{2+} influx and intracellular Ca^{2+} increase in the stimulated cell (Borde et al. 2000), whereas that of extracellular HFS is Ca^{2+}-independent (the present study).

As the pattern of discharge of STN neurons may play an important role in the physio-pathology of parkinsonism (Bergman et al. 1994; Hollerman and Grace 1992), it is tempting to correlate the present effects of in vitro HFS on the spontaneous STN activity, to the beneficial effects of high-frequency deep brain stimulation in the STN of MPTP-treated monkeys (Benazzouz et al. 1992; Hayase et al. 1996) or parkinsonian patients (Benabid et al. 1994; Limousin et al. 1998). However, such a direct correlation needs further experiments. First, clinical HFS is performed in vivo where it could affect the whole basal ganglia network, at least at the onset of stimulation. Second, clinical HFS is efficient at lower frequencies (125–185 Hz) than sometimes in vitro HFS does. This could be explained by the differences in the characteristics of the stimulating electrode. Finally, beneficial clinical effects are observed during the continuous application of the stimulation and only for a short while after the stimulation, whereas in the present study, only events that followed the stimulation have been studied. Nevertheless, the present results give some insights in the way intrinsic activity of STN neurons can be depressed.

Present address of C. Beurrier: Dept. of Psychiatry and Behavioral Sciences, School of Medicine, Stanford University, 1201 Welch Rd., Palo Alto, CA 94304-5485.

REFERENCES

BENABID AL, POLLAK P, GROSS C, HOFFMANN D, BENAZZOUZ A, GAO DM, LAURENT A, GENTIL M, AND PERRET J. Acute and long-term effects of subthalamic nucleus stimulation in Parkinson's disease. *Stereotac Funct Neurosurg* 62: 76–84, 1994.

BENAZZOUZ A, GAO DM, PIALLAT B, BRESSAND K, AND BENABID AL. Inhibitory response of substantia nigra reticulata neurons to high frequency stimulation of the subthalamic nucleus is independent of globus pallidus activation. *Abstr Soc Neurosci* 83: 3, 1997.

BENAZZOUZ A, GROSS C, FÉGER J, BORAUD T, AND BIOULAC B. Reversal of rigidity and improvement in motor performance by subthalamic high frequency stimulation in MPTP-treated monkeys. *Eur J Neurosci* 5: 382–389, 1992.

BENAZZOUZ A, PIALLAT B, POLLAK P, AND BENABID AL. Responses of substantia nigra pars reticulata and globus pallidus complex to high frequency stimulation of the subthalamic nucleus in rats: electrophysiological data. *Neurosci Lett* 189: 77–80, 1995.

BERGMAN H, WICHMANN T, KARMON B, AND DELONG MR. The primate subthalamic nucleus. II. Neuronal activity in the MPTP model of parkinsonism. *J Neurophysiol* 72: 507–520, 1994.

BEURRIER C, BIOULAC B, AND HAMMOND C. Slowly inactivating sodium current (INaP) underlies single-spike activity in rat subthalamic neurons. *J Neurophysiol* 83: 1951–1957, 2000.

BEURRIER C, CONGAR P, BIOULAC B, AND HAMMOND C. Subthalamic nucleus neurons switch from single-spike activity to burst-firing mode. *J Neurosci* 19: 599–609, 1999.

BEVAN MD AND WILSON CJ. Mechanisms underlying spontaneous oscillation and rhythmic firing in rat subthalamic neurons. *J Neurosci* 19: 7617–7628, 1999.

BORDE M, CAZALETS JR, AND BUNO W. Activity-dependent response depression in rat hippocampal CA1 pyramidal neurons in vitro. *J Neurophysiol* 74: 1714–1729, 2000.

BURBAUD P, GROSS C, AND BIOULAC B. Effect of subthalamic high frequency stimulation in substantia nigra pars reticulata and globus pallidus neurons in normal rats. *J Physiol (Paris)* 88: 359–361, 1994.

HAMMOND C, DENIAU JM, RIZK A, AND FEGER J. Electrophysiological demonstration of a excitatory subthalamonigral pathway in the rat. *Brain Res* 151: 235–244, 1978.

HASSANI OK, MOUROUX M, AND FEGER J. Increased subthalamic neuronal activity after nigral dopaminergic lesion independent of disinhibition via the globus pallidus. *Neuroscience* 72: 105–115, 1996.

HAYASE N, FILIION M, RICHARD H, AND BORAUD T. Electrical stimulation of the subthalamic nucleus in fully parkinsonian (MPTP) monkeys. In: *The Basal Ganglia V*, edited by Ohye C. New York: Plenum, 1996, p. 241–248.

HOLLERMAN JR AND GRACE AA. Subthalamic nucleus cell firing in the 6-OHDA-treated rat: basal activity and response to haloperidol. *Brain Res* 590: 291–299, 1992.

LIMOUSIN P, KRACK P, POLLAK P, BENAZZOUZ A, ARDOUIN C, HOFFMANN D, AND BENABID AL. Electrical stimulation of the subthalamic nucleus in advanced Parkinson's disease. *N Engl J Med* 339: 1105–1111, 1998.

NEHER E. Correction for liquid junction potentials in patch clamp experiments. *Methods Enzymol* 207: 123–131, 1992.

ROBLEDO P AND FEGER J. Excitatory influence of rat subthalamic nucleus to substantia nigra and the pallidal complex: electrophysiological data. *Brain Res* 518: 47–54, 1990.

SMITH Y AND PARENT A. Neurons of the subthalamic nucleus in primates display glutamate but not GABA immunoreactivity. *Brain Res* 453: 353–356, 1988.

VILA M, PERIER C, FEGER J, YELNIK J, FAUCHEUX B, RUBERG M, RAISMAN-VOZARI R, AGID Y, AND HIRSCH EC. Evolution of changes in neuronal activity in the subthalamic nucleus of rats with unilateral lesion of the substantia nigra assessed with metabolic and electrophysiological measurements. *Eur J Neurosci* 12: 337–344, 2000.